

Complex magnetism of lanthanide intermetallics unravelled

L. Petit,¹ D. Paudyal,² Y. Mudryk,² K. A. Gschneidner Jr.,³ V. K. Pecharsky,³ M. Lüders,¹ Z. Szotek,¹ R. Banerjee,⁴ and J. B. Staunton⁴

¹ *Daresbury Laboratory, Daresbury, Warrington WA4 4AD, UK*

² *The Ames Laboratory, US Department of Energy,
Iowa State University, Ames, Iowa 50011-3020, USA*

³ *The Ames Laboratory, US Department of Energy
and Department of Materials Science and Engineering,
Iowa State University, Ames, Iowa 50011-3020, USA*

⁴ *Department of Physics, University of Warwick, Coventry CV4 7AL, U.K.*

Abstract

We explain a profound complexity of magnetic interactions of some technologically relevant gadolinium intermetallics using an ab-initio electronic structure theory which includes disordered local moments and strong f -electron correlations. The theory correctly finds GdZn and GdCd to be simple ferromagnets and predicts a remarkably large increase of Curie temperature with pressure of $+1.5 \text{ K kbar}^{-1}$ for GdCd confirmed by our experimental measurements of $+1.6 \text{ K kbar}^{-1}$. Moreover we find the origin of a ferromagnetic-antiferromagnetic competition in GdMg manifested by non-collinear, canted magnetic order at low temperatures. Replacing 35% of the Mg atoms with Zn removes this transition in excellent agreement with longstanding experimental data.

PACS numbers:

Lanthanide compounds play an increasingly important role in the development of novel materials for high-tech applications which range from mobile phones and radiation detectors to air conditioning and renewable energies. Much of this stems from their magnetic properties, so that they are indispensable components in permanent magnets, [1] magneto-responsive devices for solid state cooling [2] and other applications. Common to all the lanthanide elements is their valence electronic structure which makes them chemically similar and also causes magnetic order. Lanthanide atoms are predominantly divalent ($5d^06s^2$ valence electron configuration), becoming mostly trivalent in a solid, donating three valence electrons to the electron glue in which the atomically-localised f -electron magnetic moments sit. The interaction between these moments derives from how the electron glue is spin-polarised. The longstanding RKKY [3] (Ruderman-Kittel-Kasuya-Yosida) free electron model of this electronic structure is typically used to try to explain the many features of the indirect coupling of the $4f$ -electron moments despite its rather poor representation of the narrow band $5d$ -states. The possible importance of the latter has already been inferred from some earlier electronic structure studies [4–7].

Whilst theoretical aspects of lanthanide magnetism are well understood at the phenomenological level, predictive first principles calculations are challenging owing to the complexities of the strongly correlated f -electrons and itinerant valence electrons along with the magnetic fluctuations generated at finite temperatures. In this letter we explore lanthanide compounds with an ab-initio theory based on Spin Density Functional Theory (SDFT) in which the self-interaction corrected (SIC) local spin density (LSD) method [8, 9] provides an adequate description of f -electron correlations [10–12] and the disordered local moment (DLM) theory [13] handles the magnetic fluctuations. We are able to give a quantitatively accurate description of the diverse magnetism of Cs-Cl (B2) ordered phases of Gd with Zn, Cd and Mg which we test against experimental data and show the complex role played by the spin-polarised valence electrons.

Local moments of fixed magnitudes are assumed to persist to high temperatures and in lanthanide compounds are formed naturally from partially occupied localised $4f$ -electron states. The orientations of these moments fluctuate slowly compared to the dynamics of the valence electrons glue surrounding them. By labelling these transverse modes by local spin polarisation axes fixed to each lanthanide atom i , $\hat{\mathbf{e}}_i$, and using a generalisation of SDFT [13](+SIC [14, 15]) for prescribed orientational arrangements, $\{\hat{\mathbf{e}}_i\}$, we can deter-

mine the *ab-initio* energy for each configuration, $\Omega\{\hat{\mathbf{e}}_i\}$ [15–19] so that the configuration’s probability at a temperature T can be found. The magnetic state of the system is set by an average over all such configurations, appropriately weighted, and specifies the magnetic order parameters, $\{\mathbf{m}_i = \langle \hat{\mathbf{e}}_i \rangle\}$, where the magnitudes $m_i = |\mathbf{m}_i|$ range from 0 for the high temperature paramagnetic (PM) (fully disordered) state to 1 when the magnetic order is complete at $T = 0\text{K}$. A distribution where the order parameters are the same on every site, $\{\mathbf{m}_i = m_f \hat{z}\}$ say, describes a ferromagnetically ordered (FM) state whereas one where the \mathbf{m}_i alternate layer by layer between $m_a \hat{x}$ and $-m_a \hat{x}$ characterises an anti-ferromagnetic (AF1) order. The free energy function $\mathcal{F}(\{\mathbf{m}_i\})$, written in terms of these magnetic order parameters, \mathbf{m}_i , monitors magnetic phase transitions. It contains the effects of the spin-polarised valence electronic structure which adapts to the type and extent of magnetic order [18, 20, 21]. For lanthanide materials DLM theory describes how valence electrons mediate the interactions between the f-electron moments. These can turn out to be RKKY-like, but can also show strong deviations from this picture as we find here for simple Gd-containing prototypes.

We start with GdZn, of particular interest in solid state cooling, [22] but also because we expect its electronic structure to be straightforward [6, 23]. The Gd atoms occupy a simple cubic lattice of the CsCl(B2) ordered phase. Our first-principles SIC-LSD calculations find the ground state Gd-ion configuration to be trivalent (Gd^{3+}), with seven localised f-states constituting a stable half-filled shell, in line with Hund’s Rules [10, 11, 18]. So Gd of all the heavy lanthanides has the relative simplicity of an S-state for its f-electrons, largely uncomplicated by crystal field effects and spin-orbit coupling. This permits a clinical look at how the interactions between large 4f-magnetic moments are mediated by the valence electrons. These come from both the lanthanide ($5d^1 6s^2$) and the post-transition metal Zn which has low-lying, nominally filled, d-shells ($3d^{10}$) added to its two s-electrons. Our *ab-initio* DLM theory can thus investigate the effect of the lanthanide 5d electrons hybridising weakly with 3d states. This touches on a very important aspect of many magnetic materials containing both rare earth and transition metal elements [24] where understanding the interplay between the localised lanthanide magnetic moments and the more itinerant magnetism originating from the transition metal d-electrons is paramount for the design of more efficient materials.

Our DLM theory calculations for the paramagnetic state of GdZn produce local moments

of magnitude $\mu \approx 7.3\mu_B$ on the Gd sites pointing in random directions so that there is no long range magnetic order, $\{\mathbf{m}_i = 0\}$. The calculated paramagnetic susceptibility [15, 16, 18], $\chi(\mathbf{q})$, with a maximum at wave-vector $\mathbf{q}_{max} = (0, 0, 0)$, shows that, in accord with experiment, GdZn develops ferromagnetic (FM) order below a Curie temperature, $T_c = 184$ K (at theoretically determined lattice constant, $a = a_{th} = 6.62$ a.u.), somewhat lower than the experimental value of $T_c = 270$ K [25] (at $a = a_{exp} = 6.81$ a.u.). We find that GdZn's T_c gradually decreases under pressure, P , with calculated $\frac{dT_c}{dP} = -0.45$ K kbar $^{-1}$ which agrees reasonably well with experimental value of -0.13 K kbar $^{-1}$ from the literature [26] (Fig.1(a)). The negative $\frac{dT_c}{dP}$ is typical of many metallic magnets owing to pressure-induced band broadening and diminished energy benefit from spin polarising the valence electrons around the Fermi energy.

Naïvely one might expect similar effects if Zn is replaced with isoelectronic Cd whose filled $4d$ -band states are simply more extended than the $3d$'s of Zn. Our calculations, however, show something rather different. Whilst both theory and experiment find GdCd to be a simple ferromagnet like GdZn, with $T_c = 234$ K ($a_{th} = 6.98$ a.u.) and 265 K [27] ($a_{exp} = 7.09$ a.u. [18]), in sharp contrast to its results for GdZn, theory predicts its T_c to increase quite dramatically with pressure (Fig.1), i.e. a positive and rather large $\frac{dT_c}{dP}$. Owing to the paucity of reliable published experimental pressure data for GdCd, [28] we have carried out measurements [18] to test this specific prediction and a comparison between the calculated and experimentally observed T_c 's for GdCd as a function of pressure is shown in Fig.1(a).

The theory-experiment agreement is excellent: $\frac{dT_c}{dP}$ from theory is $+1.5$ and from experiment is $+1.6$ K kbar $^{-1}$. Whilst not unusual for first-order magnetostructural transitions (e.g. $\approx 1-3$ K kbar $^{-1}$ is observed in $\text{Gd}_5\text{Si}_x\text{Ge}_{4-x}$ alloys [29]), this is a rather high rate for a second-order transition as occurs in GdCd. Reasons for this stark difference between GdZn and GdCd are found from our T_c calculations as a function of lattice parameter, a , (Fig.1(b)). Starting from large values, T_c initially increases with decreasing Gd-Gd distance for both GdZn and GdCd, reaching a maximum whence it starts decreasing with further reduction of the Gd-Gd distance. The $\frac{dT_c}{dP}$'s shown in Fig.1(a) originate from where the two compounds have their equilibrium lattice spacings, a_{th} , marked by blue (GdZn) and red (GdCd) arrows in Fig.1(b).

For materials with the same number of valence electrons per atom, the RKKY account of magnetic interactions would be the same. GdMg is isoelectronic with both GdZn and GdCd

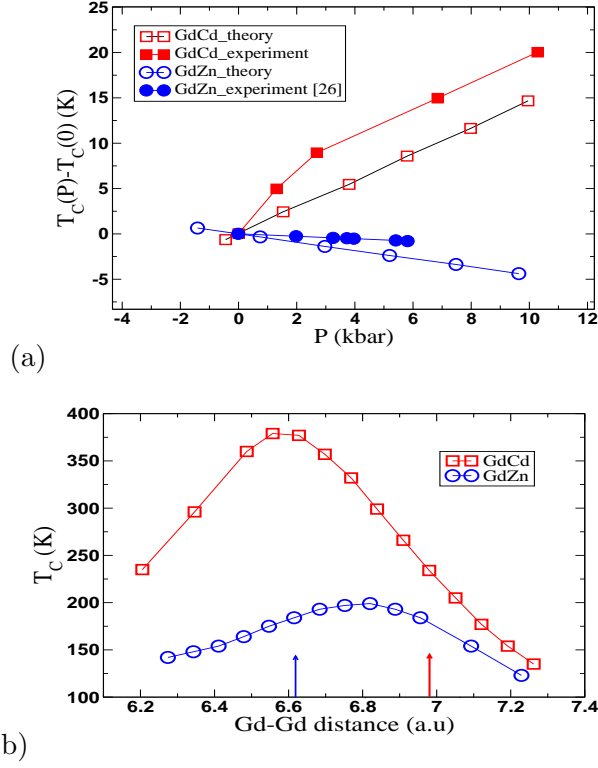


FIG. 1: (a) Comparison between theory (open symbols) and experimental [18] (filled symbols) T_c differences, $(T_c(P) - T_c(0))$, as a function of pressure, P , for GdZn (blue circles) and GdCd (red squares). The experimental data for GdZn are from Ref. (26). (b) T_c of GdZn (blue circles) and GdCd (red squares) as a function of lattice parameter a (atomic units) calculated from the theory. The vertical arrows indicate a_{th} , red for GdCd and blue for GdZn.

but with no filled 3d or 4d band of states. This difference leads to our DLM theory finding GdMg's PM state to be qualitatively different than GdZn's and GdCd's. We find a discordant blend of FM and AF1 dominant magnetic correlations in the PM state - the calculated paramagnetic $\chi(\mathbf{q})$ has two comparable peaks at wavevectors $(0, 0, 0)$ and $(0, 0, \frac{1}{2})$ [18] (in units of $\frac{2\pi}{a}$). Which one is stronger depends on the a values used. At the theory volume ($a_{th} = 7.00$ a.u. [c.f. $a_{exp} = 7.20$ a.u. [30]]), our calculations predict a FM state below $T_c = 128$ K. Reducing the Gd-Gd separation weakens the FM aspects and, for example, a 4% decrease leads to an AF1 state instead, below the Néel temperature $T_N = 87$ K.

We determine the magnetic order that evolves as T is lowered through the transition temperature to 0K as a consequence of these competing FM and AF1 effects by using our DLM theory [18] for the first time to describe a magnetically ordered state with a canted

structure and repeating the analysis for a number of a values. We set the order parameters, \mathbf{m}_i 's for the system at various stages of partial onto complete magnetic order, to alternate between $m_f \hat{z} + m_a \hat{x}$ and $m_f \hat{z} - m_a \hat{x}$ on consecutive Gd layers along the $(1, 0, 0)$ direction giving a canting angle between layers of $\Theta_c = 2 \arctan(\frac{m_a}{m_f})$ so that the overall magnetization of a system is local moment size μ ($7.3 \mu_B$) times m_f . $m_f \neq 0$, $m_a = 0$, $\Theta_c = 0$ signifies a FM state and $m_a \neq 0$, $m_f = 0$, $\Theta_c = 180^\circ$ a AF1 state.

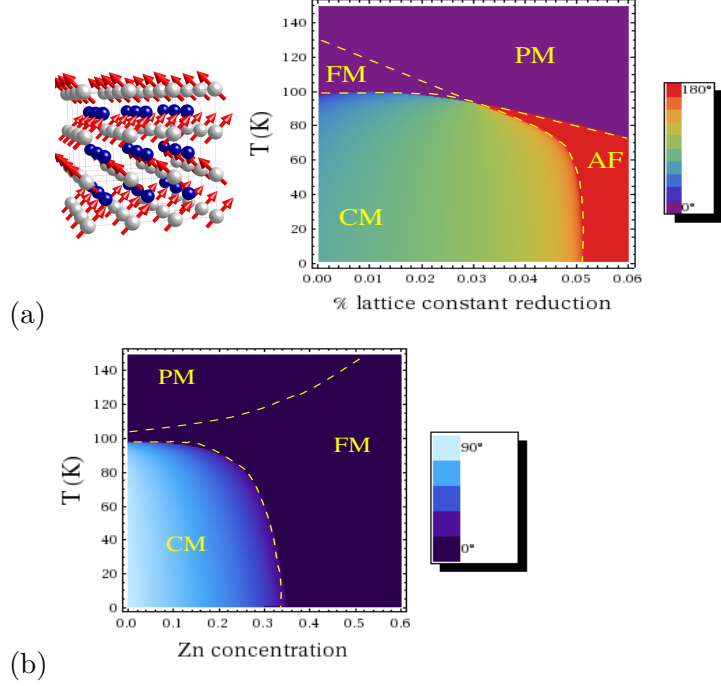


FIG. 2: (a) The magnetic phase diagram of GdMg, represented by the canting angle $\Theta_c(T)$ and its dependence on lattice spacing alongside a schematic picture of the CM state. (b) The magnetic phase diagram of $\text{GdMg}_{(1-x)}\text{Zn}_x$, $\Theta_c(T)$, and its dependence on x for a fixed lattice spacing equal to the 2% reduction value in (a), equal to a_{th} of $\text{GdMg}_{0.6}\text{Zn}_{0.4}$.

Fig.2(a) summarises our results. These are the first *ab-initio* calculations to show canted magnetism (CM) in GdMg. The figure shows the emergence of a CM from either a FM ($\Theta_c = 0$) or AF1 state ($\Theta_c = 180^\circ$). For low T , Θ_c ranges from 70° at the theoretical equilibrium lattice constant (0% reduction) through to 120° (4% reduction) before eventually forming an AF1 magnetic structure (angle 180°) with further reduction. This agrees very well with experiment [31] which finds that, upon lowering the temperature, GdMg orders into a FM state at $T_c \approx 110\text{K}$ and then undergoes a further second order transition into a

canted magnetic ordered state at $T_F \approx 85\text{K}$ [31, 32]. At low T the magnetisation $\approx 5 \mu_B$, a value we have also confirmed with our own experimental measurements. This is indicative of the FM and AF components, m_f and m_a , being roughly the same size giving a canting angle between $7 \mu_B$ -sized Gd moments of roughly 90° . This state is robust against applied magnetic fields [32] of up to 150 kOe. The experimental results are matched almost exactly by our calculations shown in Fig.2(a) for a 2 % lattice spacing reduction from a_{th} . Liu et al. [31] also found that under pressure GdMg orders into a AF1 from a PM phase at $\approx 100\text{K}$ and at a lower temperature undergoes a further first order metamagnetic transition into a canted FM phase. The authors estimated the pressure derivative of the magnetisation to be $-0.04 \mu_B \text{ kbar}^{-1}$ at 4.2K, which we have also confirmed experimentally and in fair agreement with our calculated low T value of $-0.02 \mu_B \text{ kbar}^{-1}$.

Experimentally it is known that when Gd is replaced by Tb in GdMg, there is a 1% lattice contraction [39] and a FM state undergoes a transition into a canted magnetic structure at low T with Θ_c of at least 90° . Replacing Gd with Dy leads to a larger lanthanide contraction and measurements [40] show that DyMg orders into an AF1 state, developing non-collinear structure with a FM component at low T and Θ_c of about 110° . This correlates with Fig.2(a) [18] for the smaller lattice spacing regime. The little available data for Ho-Mg [39] also indicates canted AF magnetic structure at low T . So we infer that the lanthanide contraction [15] in part causes the transition from FM-canted to AF-canted magnetic structures as the heavy lanthanide series is traversed. Our figure 2(a) also implies a tricritical point (PM-AF-FM) at some concentration, y , in the $(\text{Tb}_{1-y}\text{Dy}_y)\text{-Mg}$ alloy system with a transition to a canted structure at a marginally lower temperature or possibly a transition into a canted structure directly.

This unusual canted magnetism of GdMg is evidently destroyed by nominally filled, low-lying 3d or 4d bands from the non-lanthanide constituent. Our calculations, Fig.2(b), show what happens when a fraction x of the Mg sites in GdMg is replaced by Zn. T_c increases with x , and the low temperature canted structure vanishes altogether for $x > 0.35$. This observation is in excellent agreement with the experimental data for $\text{GdMg}_{(1-x)}\text{Zn}_x$ of Buschow et al. [33] who gave an early report of a serious shortcoming of the RKKY picture.

The successful capturing of these unusual temperature and pressure trends of the Gd intermetallics' magnetism is a consequence of the theory's detailed description of the valence electrons. The theory includes both the response of these electrons to the magnetic ordering

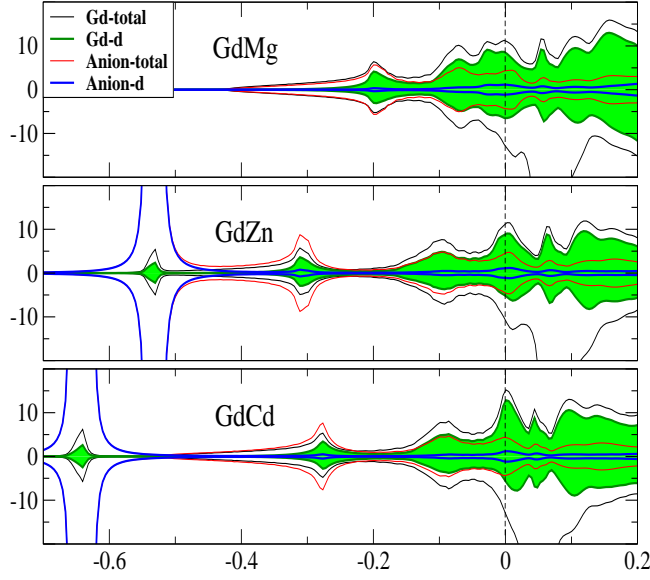


FIG. 3: The local density of states (DOS) at $a = a_{th}$ for the PM states of GdMg, GdZn and GdCd resolved into Gd (black curve) and Mg,Zn or Cd anion (red) components. The Gd d-component (green curve shaded underneath) and anion d-component (blue curve) are also shown. The upper (lower) panel shows the DOS for an electron spin-polarised parallel(anti-parallel) to the local moment on the Gd site. The total DOS, an average over all directions, is unpolarised.

of the f-electron local moments as well as their effect upon it. Fig. 3 shows the non-free electron-like PM valence density of states (DOS) of GdMg, GdZn and GdCd at a_{th} for an electron spin-polarised parallel and anti-parallel to the local moment on the Gd site [13]. Averaged over equally weighted moment orientations the DOS is unpolarised overall. Below T_c the electronic structure adjusts and spin-polarises [18] when magnetic order develops. The Gd f-moment interactions are properties of the electronic structure around the Fermi energy, ε_F . The Fermi surface (FS) of PM GdMg (for $a = 0.96a_{th}$), Fig. 4(a), shows a distinctive box structure so that a wave-vector, $(0, 0, \frac{1}{2})$, connects (nests) [36–38] large portions of parallel FS sheets and drives AF1 magnetic correlations. This topological feature is absent in GdZn’s and GdCd’s FS’s. Weak hybridization between Gd-5d and lower lying, nominally filled Zn-3d or Cd-4d states, shown in Fig. 3, causes complex differences between their electronic structures around ε_F and GdMg’s. In GdZn the Zn 3d bands are narrower than GdCd’s 4d ones and lie at slightly higher energies [18]. Moreover we find that lattice compression

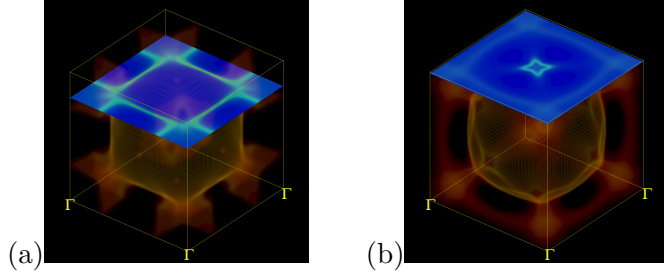


FIG. 4: The 3D Fermi surface for (a) PM GdMg ($a = 0.96a_{th}$, where Fig.2(a) shows AF1 order) which shows nesting, and (b) PM GdCd, ($a = 0.94a_{th}$, close to Fig.1(b)'s peak position) showing the 'hot spot' at wavevectors $\mathbf{k} = (\frac{1}{2}, \frac{1}{2}, 0)$. The finite width of the FS features reflect the local moment disorder.

increases Gd d-state occupation relative to sp-ones in these compounds [34, 35] which affects FS topology. In particular, as shown in Fig. 4(b) for GdCd, we find that Fig. 1(b)'s peak correlates with a distinct electronic topological transition - a 'hot spot' formed by a hole pocket around $\mathbf{k} = (\frac{1}{2}, \frac{1}{2}, 0)$, collapsing as a is reduced.

Atomically localised f-electrons and their intricate physics is inevitably the focus for lanthanide material studies. But the valence electron glue in which the f-moments sit also harbors surprises. Its s-, p- and d-electrons can shift it far from a nearly free electron model, as exemplified by the canted magnetism of GdMg and the stark contrast of the magnetism of isoelectronic GdZn and GdCd with their disparate pressure variations. The predictive *ab-initio* computational modelling described here has successfully accounted for the subtle aspects of the valence electrons' spin polarisability around ε_F and how it is affected by occupation of lower-lying lanthanide-other metal d-electron bonding states. This implies that further successful quantitative modelling of the rich variety of technologically useful lanthanide-transition metal materials must also treat valence electronic structure accurately and in quantitative detail. We have shown that coordinated *ab-initio* theory-experimental studies have the capability of producing new guidelines for understanding the magnetism in lanthanide-transition metal magnets. Factors such as the average number of valence electrons or band-filling, separation in energy of the lanthanide 5d and the other constituents' d-bands and the valence band widths, reminiscent of the modern analogs of the famous Hume-Rothery rules [41] for alloy phase stability, will influence the nature of the valence electron structure around ε_F and the magnetism it supports.

Acknowledgements

We acknowledge the late W.M. Temmerman for valuable and insightful discussions during the early stages of this work. The work was supported by the UK EPSRC by Grant No. EP/J06750/1 and an EPSRC service level agreement with the Scientific Computing Department of STFC. Work at Ames Laboratory was supported by the Materials Sciences and Engineering Division of the Office of Basic Energy Sciences of the U.S. Department of Energy under contract no. DE-AC02-07CH11358 with Iowa State University.

-
- [1] E. Burzo, Rep. Prog. Phys. **61**(9):1099-1266,(1998).
 - [2] K.A. Gschneidner Jr., L.R. Eyring, J.-C. Bünzli and V.K. Pecharsky, Eds.: Handbook on the Physics and Chemistry of the Rare Earths, vols.1-45, (Elsevier, 1978-2015).
 - [3] T. Kasuya, Prog. Theo. Phys. **16**(1), 45-57, (1956).
 - [4] I.A. Campbell, J. Phys. F Met. Phys. **2**(3),L47-50, (1972).
 - [5] A.V. Postnikov, V.P. Antropov and O. Jepsen, J, Phys. Condens. Matter **4**(10),2475-2486, (1992).
 - [6] K.H.J. Buschow et al., J. Alloys Compd. **244**,113-120, (1996).
 - [7] S. Khmelevskiy, I. Turek and P. Mohn, Phys. Rev. B**70**, 132401, (2004).
 - [8] J.P. Perdew and A. Zunger, Phys. Rev. B **23**(10),5048-5079, (1981).
 - [9] M. R. Pederson, R. A. Heaton, and C. C. Lin, J.Chem. Phys. **82**, 2688 (1985).
 - [10] P. Strange, A. Svane, W.M. Temmerman, Z. Szotek and H. Winter, Nature **399**(6738),756-758,(1999).
 - [11] L. Petit, R. Tyer, Z. Szotek, W.M. Temmerman and A. Svane, New J. Phys. **12**, 113041, (2010).
 - [12] L. Petit et al., J. Phys. Condens. Matter **13**(38),8697-8706, (2001).
 - [13] B.L. Gyorffy, A.J. Pindor, J.B. Staunton, G.M. Stocks and H. Winter, J. Phys. F Met. Phys. **15**(6),1337-1386, (1985).
 - [14] M. Lüders et al. Phys. Rev. B**71**(20),205109,(2005).
 - [15] I.D. Hughes et al., Nature **446**(7136),650-653, (2007).
 - [16] J.B. Staunton and B.L. Gyorffy, Phys. Rev. Lett. **69**(2),371-374, (1992).

- [17] J.B. Staunton et al., Phys. Rev. B **74**(14),144411, (2006).
- [18] Online supplementary information:
- [19] J.B. Staunton, A. Marmodoro and A. Ernst, J. Phys. Condens. Matter **26**(27),274210, (2014).
- [20] J.B. Staunton, R. Banerjee, M. dos Santos Dias, A. Deak, L. Szunyogh, Phys Rev B **89**(5),054427, (2014).
- [21] J.B. Staunton, M. dos Santos Dias, J. Peace, Z. Gercsi and K.G. Sandeman, Phys. Rev. B **87**(6),060404(R),(2013).
- [22] V.K. Pecharsky and K.A. Gschneidner Jr., Cryocoolers **10**,629 (2002).
- [23] J. Rusz, I. Turek and M. Diviš, J. Alloys Compd. **408-412**,930-933, (2006).
- [24] B. Sanyal et al., Phys. Rev. Lett. **104**, 156402 (2010).
- [25] K. Kanematsu, G.T. Alfieri and E. Banks, J. Phys. Soc. Jpn. **26**(2),244-248, (1969).
- [26] T. Hiraoka, J. Phys. Soc. Jpn. **37**(5),1238-1241, (1974).
- [27] G.T. Alfieri GT, E. Banks E, K. Kanematsu and T. Ohoyama, J. Phys. Soc. Jpn. **23**(3),507-510, (1967).
- [28] K.H.J. Buschow et al., Physica B **237-238**,570-571, (1997).
- [29] Y.C. Tseng et al., Phys. Rev. B **76**(1),014411, (2007).
- [30] P. Manfrinetti and K.A. Gschneidner Jr., J. Less-common Met.**123**, 267, (1986).
- [31] M.L. Liu, M. Kurisu, H. Kadomatsu and H. Fujiwara, J. Phys. Soc. Jpn. **55**(1),33-36, (1986).
- [32] P. Morin, J. Pierre, D. Schmitt and D. Givord, Phys. Lett. A **65**(2),156-158, (1978).
- [33] K.H.J. Buschow and A. Oppelt, J. Phys. F Met. Phys. **4**(8),1246-1255, (1974).
- [34] D.G.Pettifor, Bonding and Structure of Molecules and Solids, Oxford University Press, (1995).
- [35] G.E. Grechnev, A.S. Panfilov, I.V. Svechkarev, K.H.J. Buschow and A. Czopnik, J. Alloys Compd. **226**, 107, (1995).
- [36] L.M. Roth, H.J. Zeiger and T.A. Kaplan, Phys. Rev. **149**, 519, (1966).
- [37] S. Dugdale, Low Temperature Physics **40**, 328-338, (2014).
- [38] K.M. Dobrich et al., Phys. Rev. Lett. **104**, 246401, (2010).
- [39] R. Aleonard R, P. Morin P, J. Pierre J and D. Schmitt, J. Phys. F Met. Phys. **6**(7),1361-1373, (1976).
- [40] M. Belakhovsky M, J. Chappert and D. Schmitt, J. Phys. C Solid State **10**(17),L493-497, (1977).
- [41] Alloy Phase Stability, eds. G. M. Stocks and A. Gonis, NATO ASI Series **163**, (1989).